Ecotoxicology and Environmental Safety 190 (2020) 110088

Contents lists available at ScienceDirect

Ecotoxicology and Environmental Safety

journal homepage: www.elsevier.com/locate/ecoenv

Advanced sensing platform for electrochemical monitoring of the environmental toxin; bisphenol A

Hoda Ezoji[a], Mostafa Rahimnejad[a,*], Ghasem Najafpour-Darzi[b]

[a] Biofuel and Renewable Energy Research Center, Department of Chemical Engineering, Babol Noshirvani University of Technology, Babol, 47148-71167, Iran
[b] Biotechnology Research Laboratory, Faculty of Chemical Engineering, Babol Noshirvani University of Technology, Babol, Iran

ARTICLE INFO

Keywords:
Environment
Bisphenol A
Electrochemical sensor
Carbon nanotube
Titanium dioxide

ABSTRACT

Environmental xenoestrogen, Bisphenol A (BPA), is a vitally important industrial raw chemical which can bring about a wide variety of adverse impacts on our health and environment. Therefore, it is imperative to develop efficacious systems to measure BPA and improve the life quality. Herein, a mixture of titanium dioxide nanoparticles (TiO_2NPs) and glutaraldehyde cross-linked chitosan (GA-CS) loaded into a carbon nanotubes paste matrix to construct a novel electrochemical sensor (TiO_2NPs/GA-CS/CNTPE) with a synergetic intensified current signal for the quantitative analysis of BPA. The surface morphology of the modified sensor was assessed by field emission scanning electron microscope (FESEM), X-ray diffraction (XRD) and energy dispersive X-ray spectroscopy (EDX). The prepared TiO2NPs/GA-CS/CNTPE displayed increased electrocatalytic activity toward BPA. The calibration curve of BPA shows linear response in the BPA concentration range of 0.01–6 μM with the lowest limit of detection of 9.58 nM (S/N = 3). The sensor exhibited high sensitivity and selectivity, good reproducibility, desirable stability and excellent performance in detection of BPA in real samples, which prove that TiO2NPs/GA-CS/CNTPE is quite applicable for food, medical and environmental analyses.

1. Introduction

Over the preceding decades, a considerable enhancement in presence of hazardous and deleterious chemicals in human and wildlife environment has become a controversial issue and drawn a lot of attention. A class of these critical substances which may modulate or disrupt the human and animal endocrine hormonal system are termed as endocrine disrupting compounds (EDCs) (Wooding et al., 2017). They are a group of bio-accumulative and resistant environmental exposures with various physico-chemical attributes that can trigger a potential risk for the wellness of human and wildlife through diverse exposure routes. Main sources of EDCs consist of phthalates, pesticides, hormones, polychlorinated biphenyls, dioxins, personal care products and pharmaceuticals. Analysis of EDCs is challenging since they are made up of a broad group of chemicals that are pervasive at trace amounts in our surroundings (Annamalai and Namasivayam, 2015; Chang et al., 2009; Petrovic et al., 2002; Trenholm et al., 2006). Among these xenobiotics, Bisphenol A (BPA; 2,2-bis (4-hydroxyphenyl) propane) (Scheme 1) as one of the most important EDCs, have emerged as a crucial public health matter. As well as the other EDCs, BPA and its analogues are prevalent in our environment (Jensen et al., 2019). This environmental oestrogen has been produced and employed in very large quantities as a monomer or additive in the fabrication of epoxy resins, polycarbonate plastics and other polymeric products. Subsequently, as a key constituent of plastics, BPA is broadly discovered in some of household products, namely, nursing bottles, food containers, thermal papers, beverage vessels, dental sealants, medical equipment and children's plastic toys (Xue et al., 2017). As a consequence, it is commonly determined in human blood, urine and breast milk by virtue of low but persistent exposure (Zou et al., 2019). Additionally, BPA has been mentioned as an EDC by cause of its genotoxic and estrogenic activity. Moreover, it has been considered to be associated with the appearance of diverse health impacts such as infertility, diabetes, birth defects, cardiovascular disease and developmental neurotoxicity. More importantly, BPA may cause enhancement in incidence of some kinds of cancers (Maffini et al., 2006; Di Donato et al., 2017). All the above-mentioned outcomes have resulted in increasing concerns toward environmental contamination. Therefore, authoritative, sensitive and efficient methods for detecting trace levels of BPA in the biological, industrial, environmental and soil samples are seriously required (Shi et al., 2017). Up until now, for sensitive determination of BPA, a large number of conventional systems based on spectrophotometry (Zhang et al., 2016), chemiluminescence detection (Maiolini et al., 2014), fluorescence (Mo et al., 2017), immunoassay (Hou et al., 2016), laser

* Corresponding author.
E-mail addresses: ezojihoda@yahoo.com (H. Ezoji), Rahimnejad@nit.ac.ir (M. Rahimnejad), najafpour@nit.ac.ir (G. Najafpour-Darzi).

https://doi.org/10.1016/j.ecoenv.2019.110088
Received 29 October 2019; Received in revised form 8 December 2019; Accepted 11 December 2019

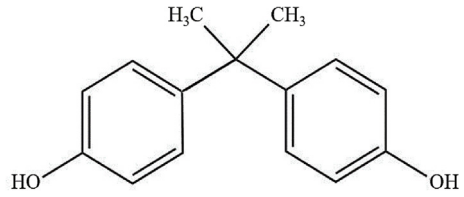

Scheme. 1. Schematic molecular structure of BPA.

direct writing (Cheng et al., 2016), chromatography methods (Deceuninck et al., 2015) and surface-enhanced Raman scattering (SERS) (Chung et al., 2015) have been reported. In spite of the fact that the afore-mentioned approaches are efficient enough for detection of BPA, they still suffer from several drawbacks. Long examination time, high-priced and sophisticated apparatus, advanced preparation procedures and well-trained experts are examples of difficulties which limit their usages (Güney and Güney, 2017; Yola et al., 2014). By contrast, currently, electrochemical techniques, in consideration of superior characteristics, e.g., on-site assay, time-saving, portability, validity, simplicity, excellent accuracy, high selectivity and sensitivity and low-cost instrumentations, attained to a supreme research enthusiasm. What is more, BPA is an electroactive chemical due to its phenolic hydroxyl agents. Thus, innumerable electrochemical systems have been proposed for detection of BPA based on its oxidation reaction signal at the surface of electrodes. Nevertheless, the response signal of bare electrodes is quite weak as a result of the insignificant electron transfer between BPA and the sensing interface. To address this issue, developing modified electrodes using advanced materials with large surface area, good adsorption, desirable electron transfer capability and excellent electrical conductivity is still a challenging matter (Liu et al., 2017; Yin et al., 2010). To this end, carbon nanostructures are recognized as the promising materials for applying in construction of electrochemical sensors and biosensors (Zhu et al., 2014; Alwarappan et al., 2009).

Amidst these beneficial materials, carbon nanotubes (CNTs), one of the most important carbon allotropes, presenting an array of unprecedented attributes which include high rate of electron transfer, peerless structure, broad potential window, high chemical stability, large surface area, desirable electrical conductivity, excellent electrocatalytic activity and advanced mechanical strength. Furthermore, CNTs can be merged with other superior materials to promote the performance of sensors in respect of specificity and sensitivity (Kumar et al., 2017; Miodek et al., 2015).

Based on the foregoing, metal and metal oxides nanoparticles in integration with CNTs can improve the performance of analytical instruments. Among these nanoscale materials, transition metal oxides (TMOs) display better function due to their semi-conductor features. They have various types of outstanding properties as improved electrocatalytic activity and large surface area (Sedghi et al., 2015; Rahman et al., 2010). In the midst of them, titanium dioxide nanoparticles (TiO_2NPs) have exceptional characteristics, such as bio-compatibility, stability, non-toxicity, high conductivity, favorable adsorption ability, cost affordability and high surface area. In the interest of these exceptional characteristics of nano-sized TiO_2, it became a criterion over the other ones (Arkan et al., 2017; Demir et al., 2014).

Chitosan (CS), a chitin industrial derivative, is a polysaccharide biopolymer which has drawn massive interest in fundamental science, industrial biotechnology and applied research. For several decades, it has been broadly applied in molecular separation, artificial skin, water treatment, bone substitutes, food packaging film and so on. Nowadays, by virtue of its considerable functional and structural properties such as sufficient film-forming ability, multiple functional factors, biodegradability, biocompatibility, low toxicity, chemical inertness and hydrophilicity, innumerable processes have been conducted on applying CS in wide range of sensing and biosensing applications. In combination with CNTs, CS can enhance the hydrophilicity of these nanomaterials in order to facilitate and improve the adsorptive, covalent and ionic bindings with analytes. Furthermore, simultaneous utilization of CNTs and CS can create a mixture with superior mechanical and electrochemical features versus to CNTs or CS. Some functionalities of CS can be better by chemical or physical modification. In this respect, glutaraldehyde (GA) is a covalent cross-linking agent which can improve CS mechanical properties, fixes the polymer structure and corrects the permeation (Fowotade et al., 2019; Wu et al., 2018; Li et al., 2013; Purnaratrie, 2015).

The present research seeks to elucidate a new systematic attempt to establish a novel approach at the confluence between electrochemistry and nanotechnology to develop a promising sensing device based on CNTs paste electrode (CNTPE) modified with TiO_2NPs and cross-linked CS. The proposed electrochemical sensor has been coupled with cyclic voltammetry (CV), differential pulse voltammetry (DPV) and electrochemical impedance spectroscopy (EIS) to evaluate the electrochemical response of BPA on the electrode and demonstrated excellent sensitivity and reproducibility. We were convinced that the major advantages of the developed sensor lie in the unique properties of the applied nanomaterials and CS and the synergic effects of them. To realize the sensing manner of the modified electrode, diverse investigations contain sensitivity, selectivity, limit of detection, effect of interferences on detection, reproducibility and stability were performed. It is of great importance to emphasize that the monitoring examinations conducted in this study are on the basis of the analyses of real samples, which would be suitable for medical and environmental screening targets.

2. Experimental

2.1. Materials and reagents

BPA was supplied by Sigma-Aldrich and utilized as received. CNT was purchased from Neutrino. TiO_2NPs, graphite powder and CS were obtained from Sigma-Aldrich. All other chemicals employed in this research were provided from regular sources and applied immediately after receipt without any excess purification. BPA 10^{-2} M stock solution was prepared by dissolution in methanol (HPLC grade) obtained from Merck and diluted to desired concentration by phosphate buffer solution (*PBS*, 1 M, pH 7). *PBS* solutions as supporting electrolyte were prepared with various pH by mixing the stock solution of KH_2PO_4 and K_2HPO_4. Afterwards, the solutions pH values were adjusted by NaOH (1 M) or HCl (1 M). Finally, BPA and PBS stock solutions were kept at 4 °C prior to use.

2.2. Instruments and characterization

The electrochemical examinations were performed using a computer-controlled Ivium Vertex workstation (IVIUM Technologies) with a conventional three-electrode system, which uses TiO2NPs/GA-CS/CNTPE as working electrode, an Ag/AgCl reference electrode and a platinum wire counter electrode. Field emission scanning electron microscope (FESEM) images were collected on a FEI Nova NanoSEM 450. X-ray diffraction analyses were performed by Rigaku Ultima IV X-Ray Diffractometer. Energy dispersive X-ray spectroscopy (EDX) patterns were taken using a BRUKER X Flash 61 10.

2.3. Preparation of GA cross-linked CS

The cross-linking reaction as the chemical modification was conducted on via suspending 1.5 gr CS in 25 ml of cross-linking agent aqueous solution (2.5% (w/v)). The resulting suspension was subjected to constant and persistent stirring at ambient temperature for 12 h. Afterwards, the as-prepared GA cross-linked CS was filtered. In order to eliminate the unreacted GA, the filtrate was rinsed with double distilled water and dried at room temperature. The final dried product was used to modify the bare electrode (Vieira et al., 2006).

2.4. Fabrication of bare and modified working electrodes

The schematic illustration of the step-by-step preparation process of the modified electrochemical sensor is shown in Scheme S1. The unmodified CNTPE was prepared by blending and grinding CNTs with mineral oil in a mortar. The final mixture was homogenized for about 30 min, manually. Subsequently, the product was pressed into the glass electrode body and a copper wire embedded into the electrode, served as electrical connection. Prior to use, in order to obtain a smooth and fresh surface, the CNTPE was polished against a clean weighing paper.

The chemically modified electrodes were also constructed in the same way as explained above via adding sufficient amount of the modifiers to the afore-said mixture.

2.5. Experimental procedures

The basic features of the fabricated electrochemical sensor were mainly determined using CV while DPV was carried out in order to measure the level of BPA in standard and real samples. The CV curves were recorded in the potential range of 0–1 V at the scan rate of 50 mV s^{-1}. Differential pulse voltammograms were collected with the potential range of 0.2–1 V. All the afore-mentioned electrochemical measurements were performed in 0.1 M PBS (pH 7) containing certain amount of BPA and 0.1 M NaCl.

The charge transfer resistance (R_{ct}) and electronic characteristics of the proposed sensor were evaluated applying EIS via plunging the electrode into PBS (pH 7) containing $[Fe(CN)_6]^{3-/4-}$ redox couple over the frequency range of 10 mHz–100 kHz at the scan rate of 50 mV s^{-1}. Moreover, CV tests in $[Fe(CN)_6]^{3-/4-}$ solution were employed with the scan rate of 50 mV s^{-1} and the potential was swept from −0.2 to 0.8 V. All the experiments were conducted on in ambient condition.

2.6. Sample preparation

All the water samples consist of river (Sardab Rood) water and tap water were gathered in laboratory and directly utilized without any treatment. The other samples include baby bottle and drinking bottle were supplied from local markets and used to study BPA oral intake. Initially, all the samples were cut into tiny portions and sonicated in the mixture of water and acetone. Thereafter, certain amounts of each sample were put into ethanol and kept at 80 °C for 48 h. Then, the mixture was cooled and filtered. The filtrate was kept in a volumetric flask (100 ml) and stored at 4 °C. Prior to analysis, the as-prepared sample was diluted with PBS (pH 7).

3. Results and discussion

3.1. Morphological and component characterization

Composition, structure and morphological characteristics of electrode materials can remarkably affect the electrochemical study. Thence, initially, the structure of crystal phase of CS and GA-CS were assessed by XRD. According to Fig. S1, the difference between the non-cross-linked and GA cross-linked CS is quite clear in powder XRD spectra. Two diffraction peaks in XRD spectrum of pure chitosan reveal the semi-crystalline character of this polymer. CS high crystallinity is a result of numerous amine and hydroxyl groups in its structure which can form strong hydrogen bonds. By comparison, after cross-linking of CS with GA, by cause of the hydrogen bond deformation in consideration of the replacement of the functional groups, its rigid structure weakens, the polymer crystallinity decreases and its amorphous character increases. So, the broad peak in XRD pattern of the cross-linked CS confirm that the sample is changing from the crystalline nature to amorphous one. Elemental analysis, EDX, provides the composition of CS and GA cross-linked CS (Figs. S2 and 3). As can be observed, there is a difference in amounts of elements between pure and cross-linked CS. These variations in contents of elements clearly confirm the successful cross-linking process.

Aiming to achieve a better insight into the various stages of electrode modifications, FESEM imaging was carried out. FESEM micrographs of pristine CNTPE is illustrated in Fig. S4a. The tubular structure of CNTs can be observed which are homogeneously distributed all over the paste. According to the intact structure of CNTs, it can be deduced that the process of blending does not damage the tubes. More importantly, this unique structure as well as the excellent surface area of CNTs, could enhance the rate of electron transfer and improve the electrochemical output signal. Fig. S4b, shows the FESEM image of TiO_2NPs/CNTPE. As is clear lots of spherical TiO_2NPs are well spread all over the paste, suggesting more active surface area. In Fig. S4c, it can be seen that the GA cross-linked CS particles are compactly dispersed in CNT paste, which could enhance the roughness and effective surface area. In comparison, by simultaneous incorporation of TiO_2NPs and GA cross-linked CS into CNT paste matrix (Fig. S4d), the uniform distribution of modifiers, present more effective area to further enhance the sensitivity of sensor.

3.2. Electrochemical evaluation of various modified interfaces

3.2.1. CV

CV is an efficient and important technique, which can provide information on the charge transfer properties of the bare and modified sensors. Fig. 1a, presented the outcomes of CV scans exposed different electrodes including bare CNTPE and GA-CS/CNTPE, TiO_2NPs/CNTPE and TiO_2NPs/GA-CS/CNTPE. The CV analyses were performed by $[Fe(CN)_6]^{3-/4-}$ as redox probe. As can be seen, it is evident that modification of CNTPE increases the peak current by virtue of the enlarged electrode surface area and accelerated electron transfer kinetics. More specifically, at pristine CNTPE, the redox signal consists of a couple of cathodic and anodic peaks with the difference between the peak potentials (ΔE_p) of 0.12 V. Compared with the unmodified working electrode, for GA-CS/CNTPE, the electrochemical peak current and redox reversibility were improved, indicating the improvement of electron transfer between the redox probe and working electrode. At the next step, in modification with TiO_2NPs, the current intensity increased while ΔE_p decreased, demonstrating that the conductivity was elevated. This phenomenon could be attributed to the exceptional properties of TiO_2NPs such as adequate electrochemical activity, large surface area and high conductivity. As expected, simultaneous introduction of TiO_2NPs and GA-CS further raises the peak current and decreases ΔE_p. These observations suggest an increment in electrocatalytic activity and the rate of electron transfer by cause of the synergistic effects of modifiers. What's more, it can be concluded that simultaneous incorporation of TiO_2NPs and GA-CS into CNTPE can provide sufficient pathways for electron transfer at the electrochemical sensor – electrolyte interface.

3.2.2. EIS

EIS is a functional tool to verify the interfacial and electron transport characteristics of differentially surface-modified electrodes. In order to perform EIS, as well as the CV tests, an electrochemical cell containing $[Fe(CN)_6]^{3-/4-}$ as redox probe was applied. The EIS corresponding data are displayed as Nyquist plots. A Nyquist plot is made up of two portions, a semi-circle at high frequency region, represents the electron transfer limited process followed by a linear portion normally seen at lower frequencies ascribes to the mass transfer process. The diameter of the high frequency semi-circle directly points to the resistance to electron transfer (R_{ct}). Fig. 1b, illustrated the Nyquist diagram of EIS spectra gained at different electrodes. As shown, the EIS spectra present approximately linear line in all frequency ranges, which can be related to the CNT unique electrical characteristics that led to development of charge transfer pathways. Moreover, as already mentioned, this phenomenon implies that the electrode reactions are of

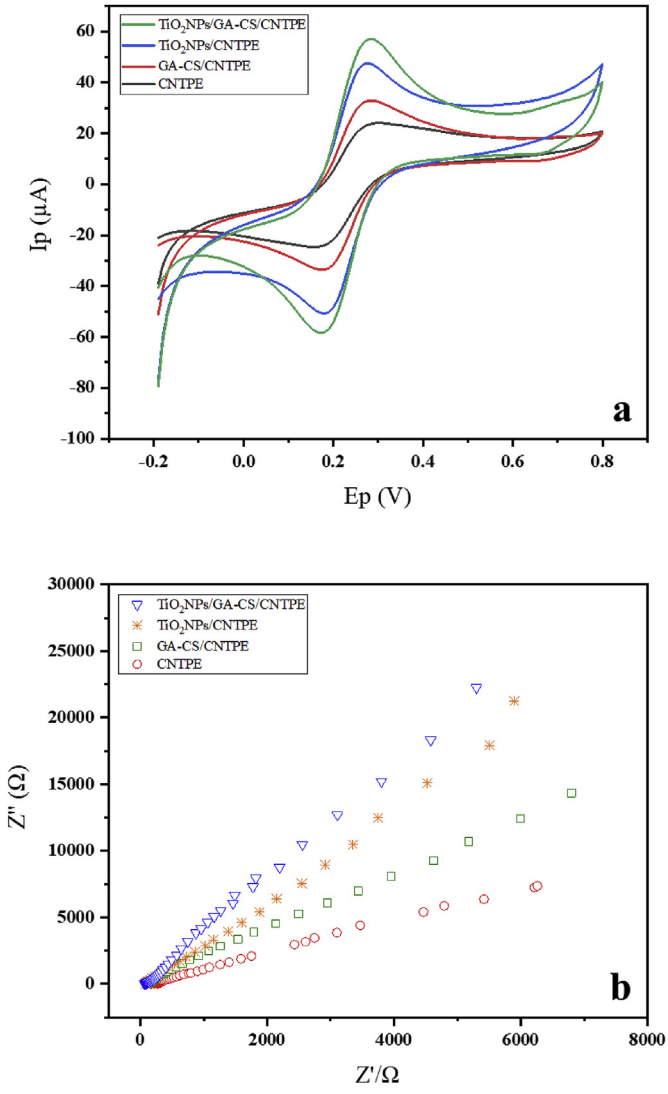

Fig. 1. CVs (**a**) and Nyquist plots (within the frequency range of 10^{-2} to 10^{5} Hz) (b) of bare and modified electrodes in 5 mM $[Fe(CN)_6]^{3-/4-}$ containing 20 mM NaCl.

diffusion controlled ones. Nevertheless, the lowest value of R_{ct} was obtained for TiO_2NPs/GA-CS/CNTPE as compared to the other controlled working electrodes, probably due to the enhanced surface area, improved conductivity and facilitated transport of electrons since integration of modifiers. Thus, results pointed out that EIS outcomes are consistent with that of CV.

3.3. Electrochemical performance of BPA on diverse electrodes

As mentioned before, BPA is an electroactive compound. Thus, for the purpose of probing its redox behavior, also assessing the capability of modifiers to ameliorate the electrode performance for BPA detection, the CVs were recorded at the surfaces of different electrodes. The obtained voltammograms are presented in Fig. 2. All electrodes present an oxidation peak, confirming BPA electroactive nature. At the unmodified electrode, an oxidation peak appeared with poor oxidation current. By comparison, the oxidation current further increased at GA-CS/CNTPE and appeared at more positive potentials, suggesting the modifier was beneficial to improve BPA catalytic process. Moreover, TiO_2NPs/CNTPE provided a greater oxidation current, indicating that TiO_2NPs could highly raise BPA electron transfer. Obviously, TiO_2NPs/GA-CS/CNTPE showed the maximum intensity of the electrochemical signal,

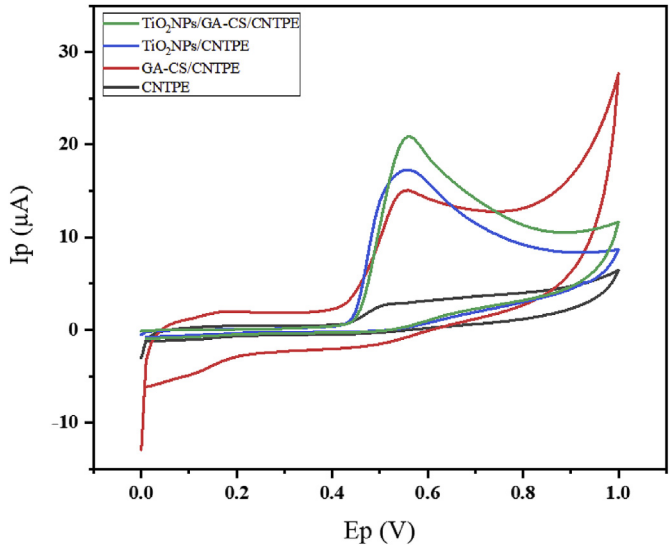

Fig. 2. CVs of unmodified and modified CNTPEs in PBS (pH 7) containing 10^{-4} M BPA and 20 mM NaCl.

demonstrating that GA-CS and TiO_2NPs combination exhibited higher electro-conductivity, which could be resulted from the synergic impact and superb properties of modifiers, namely, high surface area, great electrical conductivity and much more sites for electroactive species. Furthermore, the observed shift in peak potential could be owing to the presence of modifiers that further enhance the anodic current by reducing the charge transfer resistance and enlarging the electrode effective surface area. As a consequence, simultaneous usage of modifiers in the matrix of CNTPE boosts the analyte absorption at the electrode surface which results in increase of the anodic current.

3.4. Assessment of the reaction mechanism

To investigate the electrocatalytic and the probable kinetic mechanism, the number of electrons transferred in the oxidation of 10^{-4} M BPA at TiO_2NPs/GA-CS/CNTPE was measured applying CV at various scan rates ranging from 5 to 140 mVs^{-1} (Fig. 3a). It can be clearly observed that BPA oxidation peak potentials shifted to more positive values with increasing potential sweep rate while the peak currents increased gradually with enhancing scan rates. Fig. 3b, illustrated a linear relationship between the resulted peak currents and the square root of scan rates ($\nu^{1/2}$) with the regression equation of $y = 1.5817x + 5.4434$ ($R^2 = 0.99$). This determined that a diffusion controlled process occurred at the surface of working electrode. Meanwhile, the anodic peak potential (*Ep*), as displayed in Fig. 3c, was linearly proportional to the Napierian logarithm of scan rate ($ln\ \nu$). Based on the Laviron's theory, for such an oxidation reaction, *Ep* could be expressed as the following equation (Laviron and Electrochemistry, 1974):

$$E_{pa} = E^0 + (RT/\alpha nF)\ln(RTk^0/\alpha nF) + (RT/\alpha nF)\ln \nu \quad (1)$$

where E^0, α, n, k^0, ν, F, T and R, represent formal redox potential, electron transfer coefficient, number of electron transferred, the reaction rate constant, potential scan rate, the Faraday constant, the absolute temperature and the universal gas constant, respectively. Thus, according to the calibration equation of $y = 0.0246x + 0.4253$ ($R^2 = 0.99$), the value of $RT/\alpha nF$ was equal to the slope. On the other hand, considering that for a completely irreversible electrochemical process, α is supposed to be 0.5, thus number of electrons involved in this oxidation reaction and the reaction rate constant were computed to be 2 and 4 s^{-1}, respectively.

The possible reaction mechanism of BPA at TiO_2NPs/GA-CS/CNTPE

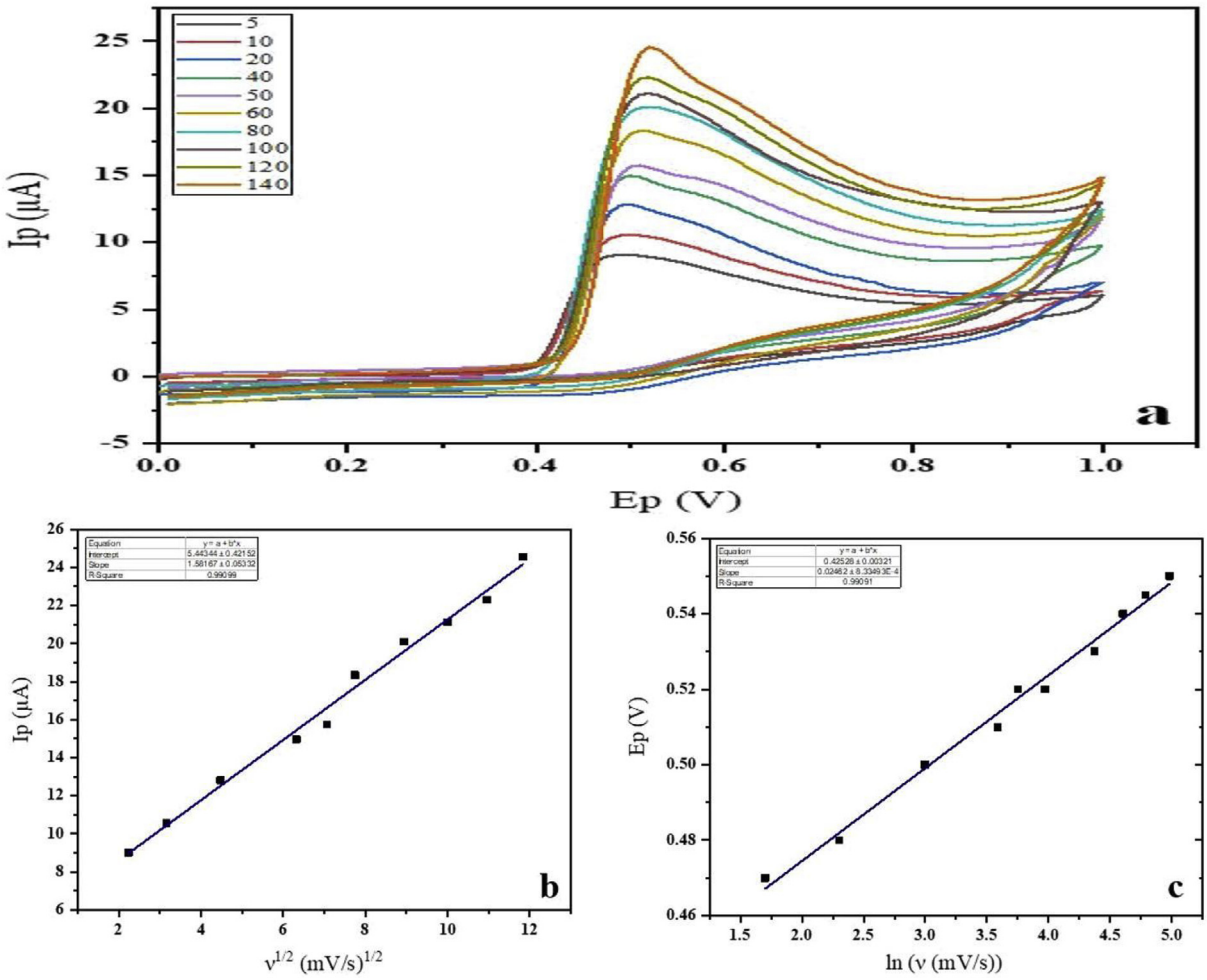

Fig. 3. CVs (**a**) of TiO_2NPs/GA-CS/CNTPE in PBS (pH 7) containing 10^{-4} M BPA and 20 mM NaCl at various scan rates from 5 to 140 mVs^{-1}, plots of *Ip* versus $\nu^{1/2}$ (**b**) and *Ep* versus *ln* ν (**c**), respectively.

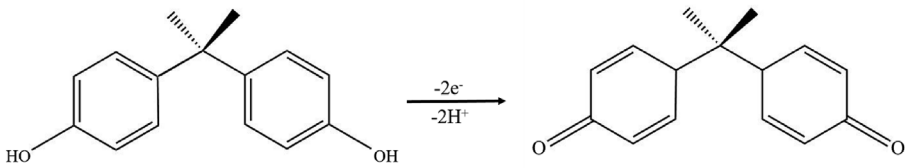

Scheme 2. Possible mechanism of BPA oxidation at TiO_2NPs/GA-CS/CNTPE.

was displayed as Scheme 2.

3.5. Studying the electrode anti-fouling capability

As previously stated, the oxidation reaction of BPA molecule was found to be an irreversible progress which results in fouling of the surfaces of electrodes. This happening is be became to the most serious difficulty within BPA oxidation owing to the electropolymerization of its phenolic groups. The oxidation polymeric products lead to the blocking of the active sites at the electrodes surfaces and delay in essential electrodes reactions. The analyte concentration is an important factor that could affect surface fouling of the electrode. In consequence, the electrocatalytic performance and anti-fouling capability of TiO_2NPs/GA-CS/CNTPE was probes toward BPA oxidation by addition of its different concentrations. As exhibited in Fig. S5a, the peak currents of BPA enhanced linearly with the increasing amounts of its concentration. In addition, the equation of the oxidation linear regression was $y = 0.0904x - 1.4995$ ($R^2 = 0.991$). Thus, these observations strongly confirm TiO_2NPs/GA-CS/CNTPE anti-fouling ability and its excellent electrochemical performance.

3.6. Effect of the supporting electrolyte pH

pH is a vitally important item which has a profound impact on the proposed sensor performance. Hereupon, the influence of buffer pH on the current response of TiO_2NPs/GA-CS/CNTPE toward 10^{-4} M BPA was examined by CV over the pH range of 3–8 (Fig. 4a). A number of well-defined anodic peaks emerged in this pH range. It is obviously observed that the peak potentials (*Ep*) and peak currents (*Ip*) changed with pH. As can be seen, the anodic peak current reached to its maximum value at pH 7. The pH in the state of the maximum current response was less than pka value for BPA (*pka = 9.73*), demonstrating that the undissociated form of BPA could be better absorbed at the surface of the modified working electrode than the dissociated one. Additionally, the anodic peak potentials linearly shifted to the negative values with increasing pH. The linear relationship could be ascribed as

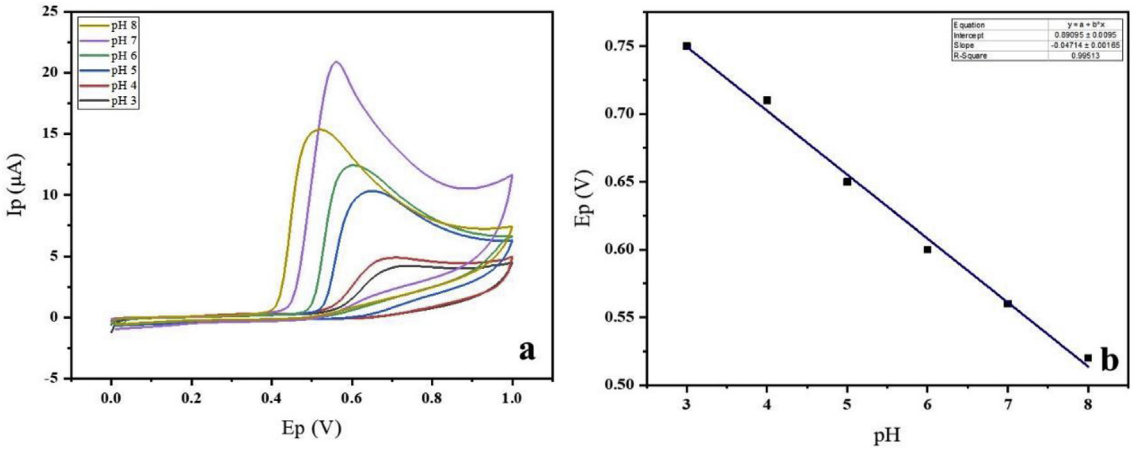

Fig. 4. CVs of TiO_2NPs/GA-CS/CNTPE recorded in 10^{-4} M BPA with various pH (**a**) and calibration plot of *Ep* versus pH (**b**).

$y = -0.0471x + 0.891$ with the supreme linearity of $R^2 = 0.9951$. The slope value between *Ep* and pH is almost close to the expected theoretical amount of 57.6 mV/pH, which means that the number of electrons and protons involved in BPA redox reaction were equal (Laviron and Electrochemistry, 1974).

3.7. Determining the electroactive surface area

Chronocoulometry (cc), a classical electrochemical step technique, is the studying of the variation of charge (coulombs) vs. time. It's a helpful approach in electrochemical studies which used to determine the electrode electrochemical active surface area. As shown in Fig. S6, chronocoulograms of 0.5 mM K_3 [$Fe(CN)_6$] reduction obtained employing different working electrodes, were assessed to compare the electroactive surface area conforming to the Anson equation (Anson, 1964):

$$Q = (2nFAD_0^{1/2}\pi^{-1/2}C_0)t^{1/2} \quad (2)$$

In the formula, Q refers to the absolute charge, n is the number of transferred electrons, F is the Faraday constant, A represents the electrode active area, C is the analyte concentration and D points to the diffusion coefficient. The electroactive surface area, A, can be obtained from the slope of the regression equation of the plot of Q versus $t^{1/2}$. Consequently, according to the slope values, largest value of electrode active area was belonged to the TiO_2NPs/GA-CS/CNTPE, which confirmed that the electroactive surface area enhanced remarkably as a result of the introduction of both of modifiers into CNTs paste. It was also found that the modifiers could improve the adsorption capacity of BPA, resulting in the enhancement of BPA current response.

3.8. Effect of the quantity of modifiers

As the amount of modifiers incorporated into the electrode can severely affect the analytical performance of the proposed sensor, effect of the quantity of the modifiers was also checked. In this sense, five electrodes consist of different amounts of TiO_2NPs (3%, 5%, 7%, 10%, 15%) were prepared and tested for detection of BPA under optimal conditions. The best results were obtained when the amount of TiO_2NPs was 10% of the whole paste. Thus, further measurements were carried out utilizing the same percent of TiO_2NPs.

In a similar way, the amount of GA-CS was also optimized. The best analytical signal was achieved for 10% of GA-CS in paste. Therefore, equal amounts of modifiers were used to enhance the sensor sensitivity.

3.9. Anti-interference capability of TiO_2NPs/GA-CS/CNTPE

Undoubtedly, the specificity of the designed electrochemical sensor is a principle practical benchmark. Therefore, to study the influence of the foreign materials as the potential interfering species, a number of organic and inorganic compounds were added to 10^{-7} M BPA solution. On the grounds of this, via measuring DPV response signal to BPA in the presence of several coexisting substances, it was found that 1000 fold concentrations of glucose, sucrose and some inorganic ions, namely, Co^{2+}, Cu^{2+}, K^+, Mg^{2+}, Na^+, Zn^{2+}, NO_3^- and SO_4^{2-} had no significant influence on BPA current response. More than that, some organic interferences which have similar structure to BPA, such as hydroquinone, p-benzoquinone, p-nitrophenol, 4-nitrophenol, nonylphenol and octylephenol were tested using the same procedure at a 500 fold higher than BPA concentration. As can be seen in Fig. S7, addition of the afore-mentioned species barely affected the BPA oxidation signal at TiO_2NPs/GA-CS/CNTPE. Ultimately, the limit of tolerance in terms of relative standard deviation (RSD) was calculated to be lower than 10%. These results denoted that TiO_2NPs/GA-CS/CNTPE had a significant anti-interference capability for various coexisting materials and an excellent selectivity for determination of BPA.

3.10. Stability, repeatability and reproducibility

With the intention of studying the reproducibility of sensor, five electrodes were independently constructed following the recommended procedure. The resulting RSD (2.8%) of the successive measurements of a certain amount of BPA using the as-prepared electrodes indicated the superior reproducibility of the working electrode. Besides, to evaluate the prepared sensor precision (repeatability), one of the afore-mentioned electrodes was employed for electrochemical determination of certain concentration of BPA for 10 consecutive times. RSD of the current responses was approximately less than 3.8, which further represented the good repeatability of the electrochemical sensor. Likewise, the impact of the sensor long-term storage was also studied. In point of fact, checking the repeatability of the above-mentioned electrode after 14 days storage in a sealed box, caused a reduction of about 4.8% in the oxidation peak current.

3.11. Sample analysis and recovery test

To testify the practical performance and feasibility of the proposed electrochemical sensor, TiO_2NPs/GA-CS/CNTPE was applied for measurement of BPA in river water, tap water, baby bottle and drinking bottle samples through a recovery assessment. Prior to test, no treatment had been carried out to the river and tap water samples except filtration using filter paper (0.45 μm). other samples were prepared pursuant to the suggested procedure in section 2.6. Under the optimal conditions, certain concentrations of BPA were spiked into the prepared samples. As listed in Table S1, the calculated RSD (n = 5) was lower

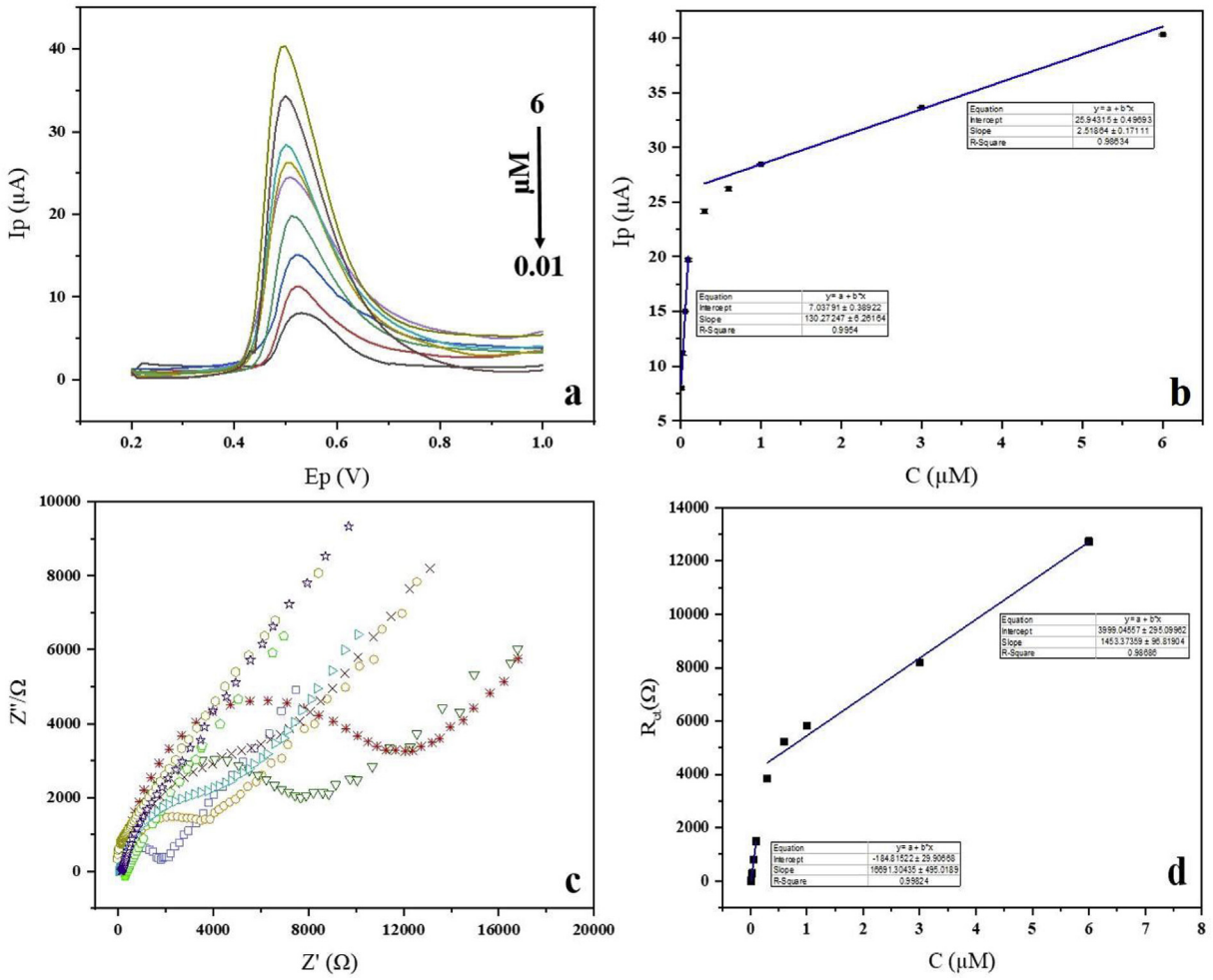

Fig. 5. DPVs of TiO_2NPs/GA-CS/CNTPE for different concentrations of BPA (**a**), the corresponding calibration curve for DPV responses (**b**), EIS spectra of TiO_2NPs/GA-CS/CNTPE for different concentrations of BPA (**c**) and the corresponding calibration curve for R_{ct} versus BPA concentration (**d**).

than 6%. Moreover, the satisfactory recovery values were obtained for BPA within the range of 94.5%–104.5%. In consequence, it can be deduced that the as-developed sensor can be effectively applied for practical analysis.

3.12. Calibration curve and BPA quantitative analysis

The changes of response currents with the analyte concentration has been found as an important approach for quantitative measurements of analytes; likewise, for computing the lowest limit of detection (LOD). In this regard, DPV is a promising technique, thanks to the merits of fast detection, excellent sensitivity and intuitive presentation of outcomes. Thus, DPV responses of TiO_2NPs/GA-CS/CNTPE toward BPA various concentrations were recorded under the optimal working conditions which can be observed in Fig. 5a. As is clear, supreme linearity of BPA DPV responses versus its concentration was attained over the range of 0.01–6 μM according to the calibration equation:

$$y = 128.75x + 7.0374 (R^2 = 0.9963)$$

The LOD of the as-prepared sensor was calculated to be 9.58 nM based on IUPAC guideline (3 s/m, where m is the calibration graph slope value and s is the blank solution standard deviation) and the limit of quantification (LOQ, 10 s/m) was estimated to be 29 nM. The performance of TiO_2NPs/GA-CS/CNTPE was compared with earlier reported BPA electrochemical sensors in Table S2. The recommended TiO_2NPs/GA-CS/CNTPE presents either relatively wider linear range or lower LOD for BPA determination. In addition, according to the discussed results, it can be concluded that the optimized electrochemical sensor can be utilized for sensitive detection of BPA content in various media.

Subsequently, this research was expanded to detect BPA by means of EIS technique. In this respect, EIS tests were performed using PBS having various concentrations of BPA ranging in 0.01–6 μM. As expected, the enhancement in the diameters of semi-circle portion of EIS spectra with addition of BPA is in perfect accordance with the efficacious detection of BPA different concentrations by the fabricated electrochemical sensor. So as to develop this method, the R_{ct} values were regressed on various concentrations of BPA to plot a calibration curve (Fig. 5d). Eventually, the LOD and LOQ of this method were calculated to be 7.012 nM and 20 nM, respectively. More importantly, the almost similar linear concentration ranges of DPV and EIS confirm the desirable performance of the proposed impedimetric method.

4. Conclusions

In conclusion, taking advantages of excellent electrical conductivity and high electrocatalytic activity, a highly sensitive electrochemical sensor has been fabricated and applied for BPA detection on the basis of CNTs paste. It should be mentioned that, as far as we know, in the present study till now, there is not any report on the determination of BPA using this combination. A competitive LOD of 9.58 nM was obtained related to a desirable concentration range. Given the simple construction of the sensor, the proposed analytical device has a promising prospect to monitor BPA occurrence in drinking water, food and

environment.

Author contribution

Hoda Ezoji: Collected the data, Performed the analysis; Mostafa Rahimnejad: Contributed data or analysis tools, Performed the analysis, Wrote the paper; Ghasem Najafpour: Other contribution.

Acknowledgements

This work was supported by the Biofuel and Renewable Energy Research Center, Department of Chemical Engineering, Babol Noshirvani University of Technology, Babol, Iran [grant number BNUT/955150002/1397]

Appendix A. Supplementary data

Supplementary data to this article can be found online at https://doi.org/10.1016/j.ecoenv.2019.110088.

References

Alwarappan, S., et al., 2009. Probing the Electrochemical Properties of Graphene Nanosheets for Biosensing Applications. pp. 8853–8857 113(20).
Annamalai, J., Namasivayam, V.J.E.i., 2015. Endocrine Disrupting Chemicals in the Atmosphere: Their Effects on Humans and Wildlife, vol. 76. pp. 78–97.
Anson, F.J.A.c., 1964. Application of Potentiostatic Current Integration to the Study of the Adsorption of Cobalt (III)-(Ethylenedinitrilo (Tetraacetate) on Mercury Electrodes. pp. 932–934 36(4).
Arkan, E., Paimard, G., Moradi, K., 2017. A Novel Electrochemical Sensor Based on Electrospun TiO2 Nanoparticles/carbon Nanofibers for Determination of Idarubicin in Biological Samples, vol. 801. pp. 480–487.
Chang, H.-S., et al., 2009. The Methods of Identification, Analysis, and Removal of Endocrine Disrupting Compounds (EDCs) in Water. pp. 1–12 172(1).
Cheng, C., et al., 2016. Bisphenol a Sensors on Polyimide Fabricated by Laser Direct Writing for Onsite River Water Monitoring at Attomolar Concentration. pp. 17784–17792 8(28).
Chung, E., et al., 2015. Surface-enhanced Raman Scattering Aptasensor for Ultrasensitive Trace Analysis of Bisphenol A, vol. 64. pp. 560–565.
Deceuninck, Y., et al., 2015. Determination of Bisphenol A and Related Substitutes/analogues in Human Breast Milk Using Gas Chromatography-Tandem Mass Spectrometry. pp. 2485–2497 407(9).
Demir, E., et al., 2014. Electrochemical Behavior of Tadalafil on TiO 2 Nanoparticles–MWCNT Composite Paste Electrode and its Determination in Pharmaceutical Dosage Forms and Human Serum Samples Using Adsorptive Stripping Square Wave Voltammetry. pp. 2709–2720 18(10).
Di Donato, M., et al., 2017. Recent Advances on Bisphenol-A and Endocrine Disruptor Effects on Human Prostate Cancer, vol. 457. pp. 35–42.
Fowotade, S.A., et al., 2019. Enhanced Electrochemical Sensing of Secondary Metabolites in Oil Palms for Early Detection of Ganoderma Boninense Based on Novel Nanoparticle-Chitosan Functionalized Multi-Walled Carbon Nanotube Platform, vol. 23. pp. 100274.
Güney, S., Güney, O.J.E., 2017. Development of an electrochemical sensor based on covalent molecular imprinting for selective determination of bisphenol-A. Electroanalysis 29 (11), 2579–2590.
Hou, C., et al., 2016. Donor/acceptor Nanoparticle Pair-Based Singlet Oxygen Channeling Homogenous Chemiluminescence Immunoassay for Quantitative Determination of Bisphenol A. pp. 8795–8804 408(30).
Jensen, T.K., et al., 2019. Prenatal Bisphenol A Exposure Is Associated with Language Development but Not with ADHD-Related Behavior in Toddlers from the Odense Child Cohort, vol. 170. pp. 398–405.
Kumar, N., Goyal, R.N.J.S., Chemical, A.B., 2017. Gold-palladium Nanoparticles Aided Electrochemically Reduced Graphene Oxide Sensor for the Simultaneous Estimation of Lomefloxacin and Amoxicillin, vol.243. pp. 658–668.
Laviron, E., Electrochemistry, I., 1974. Adsorption, autoinhibition and autocatalysis in polarography and in linear potential sweep voltammetry. J. Electroanal. Chem. Interfacial Electrochem. 52 (3), 355–393.
Li, B., et al., 2013. Synthesis, Characterization, and Antibacterial Activity of Cross-Linked Chitosan-Glutaraldehyde. pp. 1534–1552 11(5).
Liu, W., et al., 2017. Molecularly Imprinted Polymers on Graphene Oxide Surface for EIS Sensing of Testosterone, vol. 92. pp. 305–312.
Maffini, M.V., et al., 2006. Endocrine Disruptors and Reproductive Health: the Case of Bisphenol-A, vol. 254. pp. 179–186.
Maiolini, E., et al., 2014. Bisphenol A Determination in Baby Bottles by Chemiluminescence Enzyme-Linked Immunosorbent Assay, Lateral Flow Immunoassay and Liquid Chromatography Tandem Mass Spectrometry. pp. 318–324 139(1).
Miodek, A., et al., 2015. E-DNA sensor of Mycobacterium tuberculosis based on electrochemical assembly of nanomaterials. MWCNTs/PPy/PAMAM) 87 (18), 9257–9264.
Mo, R., et al., 2017. Ultrasound-Assisted Upper Liquid Microextraction Coupled to Molecular Fluorescence for Detection of Bisphenol A in Commercial Beverages. pp. 1575–1581 10(5).
Petrovic, M., et al., 2002. Recent Advances in the Mass Spectrometric Analysis Related to Endocrine Disrupting Compounds in Aquatic Environmental Samplespp. 23–51 974(1-2).
Purnaratrie, A., 2015. Comparative adsorption of Fe (III) and Cd (II) ions on glutaraldehyde crosslinked chitosan–coated cristobalite. 31 (4), 2071.
Rahman, M., et al., 2010. A Comprehensive Review of Glucose Biosensors Based on Nanostructured Metal-Oxides. pp. 4855–4886 10(5).
Sedghi, R., Pezeshkian, Z.J.S., Chemical, A.B., 2015. Fabrication of Non-enzymatic Glucose Sensor Based on Nanocomposite of MWCNTs-COOH-Poly (2-Aminothiophenol)-Au NPs, vol. 219. pp. 119–124.
Shi, R., et al., 2017. An Electrochemical Bisphenol A Sensor Based on One Step Electrochemical Reduction of Cuprous Oxide Wrapped Graphene Oxide Nanoparticles Modified Electrode, vol. 169. pp. 37–43.
Trenholm, R.A., et al., 2006. Broad Range Analysis of Endocrine Disruptors and Pharmaceuticals Using Gas Chromatography and Liquid Chromatography Tandem Mass Spectrometrypp. 1990–1998 65(11).
Vieira, R.S., et al., 2006. Interaction of Natural and Crosslinked Chitosan Membranes with Hg (II) Ions. pp. 196–207 279(1-3).
Wooding, M., Rohwer, E.R., Naudé, Y., 2017. Determination of Endocrine Disrupting Chemicals and Antiretroviral Compounds in Surface Water: a Disposable Sorptive Sampler with Comprehensive Gas Chromatography–Time-Of-Flight Mass Spectrometry and Large Volume Injection with Ultra-high Performance Liquid Chromatography–Tandem Mass Spectrometry, vol. 1496. pp. 122–132.
Wu, Z., et al., 2018. Electrochemical Nonenzymatic Sensor Based on Cetyltrimethylammonium Bromide and Chitosan Functionalized Carbon Nanotube Modified Glassy Carbon Electrode for the Determination of Hydroxymethanesulfinate in the Presence of Sulfite in Foods, vol. 259. pp. 213–218.
Xue, J., et al., 2017. Bisphenols, Benzophenones, and Bisphenol A Diglycidyl Ethers in Textiles and Infant Clothing. pp. 5279–5286 51(9).
Yin, H., et al., 2010. Sensitivity and Selectivity Determination of BPA in Real Water Samples Using PAMAM Dendrimer and CoTe Quantum Dots Modified Glassy Carbon Electrode. pp. 236–243 174(1-3).
Yola, M.L., et al., 2014. A Novel Electro Analytical Nanosensor Based on Graphene Oxide/silver Nanoparticles for Simultaneous Determination of Quercetin and Morin, vol. 120. pp. 204–211.
Zhang, R., et al., 2016. Deciphering the Toxicity of Bisphenol a to Candida Rugosa Lipase through Spectrophotometric Methods, vol. 163. pp. 40–46.
Zhu, C., et al., 2014. Electrochemical sensors and biosensors based on nanomaterials and nanostructures 87. pp. 230–249 1.
Zou, J., et al., 2019. Highly Sensitive Detection of Bisphenol A in Real Water Samples Based on In-Situ Assembled Graphene Nanoplatelets and Gold Nanoparticles Composite, vol. 145. pp. 693–702.